



Influence of K_2NbF_7 Catalyst on the Desorption Behavior of $LiAlH_4$

Nurul Amirah Ali, Noratiqah Sazelee, Muhammad Syarifuddin Yahya and Mohammad Ismail*

Energy Storage Research Group, Faculty of Ocean Engineering Technology and Informatics, Universiti Malaysia Terengganu, Terengganu, Malaysia

In this study, the modification of the desorption behavior of $LiAlH_4$ by the addition of K_2NbF_7 was explored for the first time. The addition of K_2NbF_7 causes a notable improvement in the desorption behavior of $LiAlH_4$. Upon the addition of 10 wt.% of K_2NbF_7 , the desorption temperature of $LiAlH_4$ was significantly lowered. The desorption temperature of the $LiAlH_4 + 10$ wt.% K_2NbF_7 sample was lowered to 90°C (first-stage reaction) and 149°C (second-stage reaction). Enhancement of the desorption kinetics performance with the $LiAlH_4 + 10$ wt.% K_2NbF_7 sample was substantiated, with the composite sample being able to desorb hydrogen 30 times faster than did pure $LiAlH_4$. Furthermore, with the presence of 10 wt.% K_2NbF_7 , the calculated activation energy values for the first two desorption stages were significantly reduced to 80 and 86 kJ/mol; 24 and 26 kJ/mol lower than the as-milled $LiAlH_4$. After analysis of the X-ray diffraction result, it is believed that the *in situ* formation of NbF_4 , LiF , and K or K-containing phases that appeared during the heating process promoted the amelioration of the desorption behavior of $LiAlH_4$ with the addition of K_2NbF_7 .

Keywords: hydrogen storage, lithium aluminum hydride, desorption, catalyst, metal halide

OPEN ACCESS

Edited by:

Guanglin Xia,
Fudan University, China

Reviewed by:

Xuezhong Xiao,
Zhejiang University, China
Chu Liang,
Zhejiang University of
Technology, China

*Correspondence:

Mohammad Ismail
mohammadismail@umt.edu.my

Specialty section:

This article was submitted to
Inorganic Chemistry,
a section of the journal
Frontiers in Chemistry

Received: 16 February 2020

Accepted: 01 May 2020

Published: 12 June 2020

Citation:

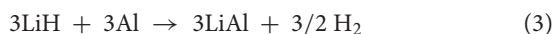
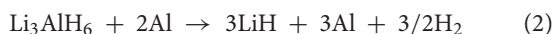
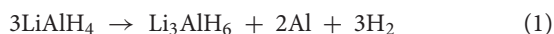
Ali NA, Sazelee N, Yahya MS and
Ismail M (2020) Influence of K_2NbF_7
Catalyst on the Desorption Behavior of
 $LiAlH_4$. *Front. Chem.* 8:457.
doi: 10.3389/fchem.2020.00457

INTRODUCTION

The excessive consumption of fossil fuels and the emission of carbon dioxide are the roots of environmental pollution. As a resolution to this global issue, the utilization of clean, and sustainable energy resources such as hydrogen, wind, and solar has become an inescapable need. Recently, hydrogen has received a large amount of attention as a future energy carrier. Hydrogen promises to be a clean and renewable energy carrier. Moreover, the production of hydrogen can be achieved from various resources, both renewable (e.g., solar, wind, and hydro) and non-renewable (e.g., natural gas and coal; Winter, 2009; Parra et al., 2019). Furthermore, energy production via hydrogen-oxygen reaction will only produce water as a by-product (Crabtree et al., 2004).

In pursuit of the success of hydrogen as a future energy carrier, the need for an efficient and reliable storage method has become the top priority. In general, there are three forms of hydrogen storage which are: (i) compressed hydrogen gas, which requires high pressure, (ii) liquefaction, and (iii) solid-state hydrogen storage via hydrides (Dalebrook et al., 2013; Zhang et al., 2016; Barthelemy et al., 2017). Solid-state hydrogen storage has been perceived to be an efficient and favorable method because of its safety, storage requirements, and storage capacity.

Lithium aluminum hydride (LiAlH₄) has major benefits and is the preferable solid-state material. LiAlH₄ is attractive due to its low temperature of hydrogen release and high storage capacity (10.6 wt.%; Andrei et al., 2005; Ares et al., 2008). The desorption process of LiAlH₄ occurs in three stages, as follows:



The first reaction (1) occurs in a temperature range of 150–175°C and desorbs 5.2 wt.% of the hydrogen. The second reaction (2) takes place at 180–220°C and desorbs 2.6 wt.% of the hydrogen, while the third reaction (3) happens at temperatures > 400°C, with 2.6 wt.% of the hydrogen desorbed.

In spite of its advantages, LiAlH₄ has some shortcomings, such as irreversible and slow desorption kinetics (Pukazhselvan et al., 2012). Moreover, the thermal decomposition in reaction 3 is considered incompatible with applied applications due to its high requirement for temperature (>400°C) to release hydrogen. Tremendous efforts have been devoted to overcoming the shortcomings of LiAlH₄, such as the implementation of the ball milling method (Balema et al., 2000, 2001; Liu et al., 2009) and impurity-doping with various catalysts such as metals (Resan et al., 2005; Xueping et al., 2009; Langmi et al., 2010; Varin and Parviz, 2012), metal oxides (Zhai et al., 2012; Li Z. et al., 2013; Li et al., 2014; Liu et al., 2014; Sulaiman and Ismail, 2017; Ali et al., 2019; Sazelee et al., 2019), Ti-based additives (Ismail et al., 2011; Amama et al., 2012; Wohlwend et al., 2012; Li L. et al., 2013), and metal halides (Fernandez et al., 2007; Suttisawat et al., 2007; Xueping et al., 2007; Sun et al., 2008; Li et al., 2012).

Among these catalysts, previous studies have revealed that metal halides provide essential catalytic effects on the performance of LiAlH₄. Cao et al. (2018) reported that the addition of ScCl₃ had a superior effect on the performance of lithium alanates. The desorption process of the LiAlH₄-10 mol% ScCl₃ sample began at a lower temperature (~120°C), while the undoped LiAlH₄ released hydrogen from around 150°C. Besides, the time needed to complete the dehydrogenation process was shortened with the addition of 1–10 mol% ScCl₃. Meanwhile, Sun et al. (2008) found that NiCl₂ significantly boosted the desorption behavior of LiAlH₄. A composite sample of LiAlH₄-NiCl₂ demonstrated three times the desorption rate of pure LiAlH₄, which was not able to desorb any hydrogen at 100°C. It was believed that the LiAlH₄-NiCl₂ sample presented this notable improvement due to the formation of Ni, which plays a vital role in accelerating the LiAlH₄-NiCl₂ system. Another investigation of the catalytic effect of metal halides was carried out by Liu et al. (2012). They proved that a LiAlH₄-TiCl₃ sample could release hydrogen at a lower temperature (80°C) than the pure LiAlH₄. Furthermore, the dehydrogenated sample had good cyclability, with the composite sample able to retain a high capacity for hydrogen (6.4 wt.%) even after completing the 3rd cycle. Moreover, Ismail et al. (2010) observed that the composite sample of LiAlH₄-1 mol NbF₅ showed a 5–6 times faster dehydrogenation rate than the milled LiAlH₄.

Additionally, the LiAlH₄-NbF₅ composite sample had lower activation energy; 67 kJ/mol (first-stage reaction) and 77 kJ/mol (second-stage reaction), respectively. However, the improvement of LiAlH₄ through the addition of a catalyst is still lacking, and further enhancements still need to be carried out. Moreover, different catalysts will enable different effects and performances. Therefore, it is interesting to enhance the desorption performance of LiAlH₄ by the addition of other metal halides.

Metal halides, especially fluorides, are known to be highly effective catalysts for solid-state materials (Sulaiman et al., 2016; Yap et al., 2017; Youn et al., 2017). A number of researchers have reported that niobium fluoride exhibits a notable effect on the hydrogenation behavior of metal hydrides and the complex hydrides. A study conducted by Luo et al. (2008) revealed that the addition of 2 mol of NbF₅ led to faster desorption kinetics for the MgH₂-NbF₅ sample as compared to pure MgH₂. At 573 K, the MgH₂-NbF₅ sample could desorb 4.7 wt.% of hydrogen, while the pristine MgH₂ desorbed almost no hydrogen. Other than that, Kou et al. (2014) added NbF₅ to LiBH₄ and demonstrated notable improvement on the desorption performance of LiBH₄. In comparison to the milled LiBH₄, which started to desorb hydrogen at >400°C, the composite sample of LiBH₄-NbF₅ had a lower desorption temperature, 60°C. Moreover, Wang and colleagues (Wang et al., 2020) showed that a composite of Mg(BH₄)₂-doped NbF₅ possessed the best dehydrogenation performance, with the ability to release hydrogen at low temperature (120°C), as compared to amorphous Mg(BH₄)₂ (126.9°C), and pristine Mg(BH₄)₂ (282.7°C). Meanwhile, Cheng et al. (2018) demonstrated that upon the addition of NbF₅, the composite of 4LiBH₄-MgH₂-Al exhibited excellent kinetics and reversibility performance. It took <4 h to achieve 90% of the total amount of hydrogen desorption. Other than that, Xiao et al. (2012) proved that the performance of LiBH₄/MgH₂ was significantly improved with the addition of NbF₅. Here, the addition of NbF₅ not only had reduced the onset decomposition temperature but also improved the dehydrogenation and absorption rates.

On the other hand, potassium (K) is another well-known additive for hydrogen storage systems. Wang et al. (2009) demonstrated that the addition of K significantly boosted the desorption process of Mg(NH₂)₂/LiH by reducing the overall reaction temperature. Furthermore, Dong et al. (2014) revealed that superior results for the hydrogenation performance of the LiH-NH₃ system were obtained by the addition of various potassium compounds.

In respect to this matter, it is interesting to mix niobium fluoride with potassium as a ternary compound in the form of K₂NbF₇ and to study its potential catalytic effect. To date, no studies have been conducted using doped K₂NbF₇ as a catalyst for LiAlH₄. Moreover, previous studies reported that K₂NbF₇ enables a remarkable improvement in the hydrogen storage performance of MgH₂ (Yahya et al., 2018; Yahya M. S. and Ismail M., 2018). Thus, it is of great interest to explore the influence of K₂NbF₇ on the desorption performances of LiAlH₄. It is anticipated that the addition of K₂NbF₇ will have notable effects on the desorption and kinetic performances of LiAlH₄.

EXPERIMENTAL DETAILS

Commercial powders of LiAlH₄ (purity 95%) and K₂NbF₇ (purity 98%) were obtained from Sigma Aldrich and were used without any modification. To minimize exposure to oxygen and water moisture, the samples were prepared and handled in the Ar-filled Mbraun Unilab glove box. In this study, 10 wt.% of K₂NbF₇ was mechanically milled together with LiAlH₄ to explore its effect on the desorption behavior of LiAlH₄. The milling process was done in a planetary ball mill (NQM-0.4) for 1 h, starting with 0.5 h of milling, followed by 6 min of rest time, and then another 0.5 h of milling in a different rotation direction at a speed of 400 rpm. The samples were placed in a hardened stainless-steel jar with four stainless balls, each 1 cm in size. The ratio of the balls to the weight of the powder was 40:1. For comparison purposes, the as-received LiAlH₄ was treated under the same conditions.

The hydrogenation performances of LiAlH₄ + 10 wt.% K₂NbF₇ were studied with temperature-programmed desorption (TPD) using Sievert-type pressure-composition-temperature (PCT) equipment (Advanced Materials Corporation). In order to determine the initial decomposition temperature, the sample was heated from room temperature to 250°C (heating rate: 5°C/min). Other than that, the desorption kinetics performances were evaluated at 90°C under 1.0 atm of pressure. The apparent activation energy, E_A , was determined using differential scanning calorimetry (DSC, Mettler Toledo, DSC/TGA 1), loading 5–7 mg of the samples into a crucible and heating from 25 to 300°C at heating ramps of 15, 20, 25, and 30°C/min under an argon flow (50 ml/min). In terms of the morphology and phase structure characterizations, the samples were analyzed using scanning electron microscopy (SEM: JEOL JSM 6350LA), X-ray diffractometry (XRD, Rigaku Miniflex), and Fourier transform infrared (IR Shimadzu Tracer-100).

RESULTS AND DISCUSSION

Figure 1 demonstrates the TPD results of the LiAlH₄ and modified LiAlH₄ system. The results show that the as-received and as-milled LiAlH₄ have similar desorption processes that occur in two stages of desorption, as in Equations (1, 2), with 7.4 wt.% hydrogen capacity. Before the ball milling process, the first stage of desorption occurred at 147°C, with 5 wt.% of hydrogen released. Meanwhile, the desorption process for the second stage was recorded to happen at around 175°C, with a capacity of 2.4 wt.% of the hydrogen. After the milling process, the initial desorption temperature of the sample was similar to that of pure LiAlH₄ but with slight temperature reductions to 144°C (first stage) and 174°C (second stage). This phenomenon showed that the 1-h milling process had an insignificant effect on the desorption behavior of LiAlH₄. In contrast, the addition of 10 wt.% of K₂NbF₇ significantly decreased the decomposition temperature for both stages, to 90 and 149°C. However, the amount of hydrogen released from the LiAlH₄ + 10 wt.% K₂NbF₇ sample was decreased to 6.3 wt.%. This is expected due to the dead weight of K₂NbF₇, which does not hold any hydrogen.

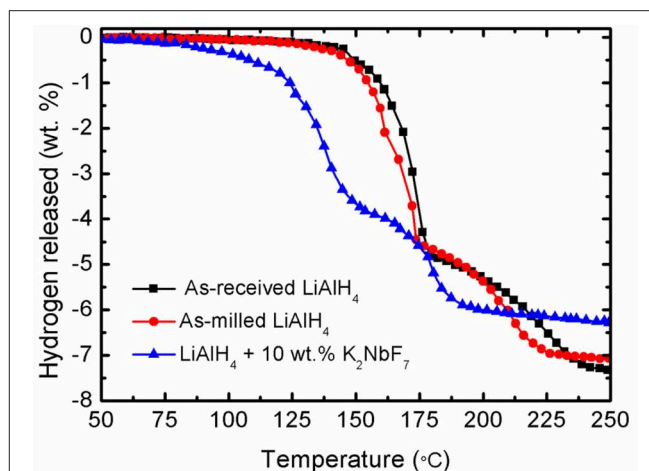


FIGURE 1 | TPD profile for the as-received LiAlH₄, as-milled LiAlH₄, and LiAlH₄ + 10 wt.% K₂NbF₇.

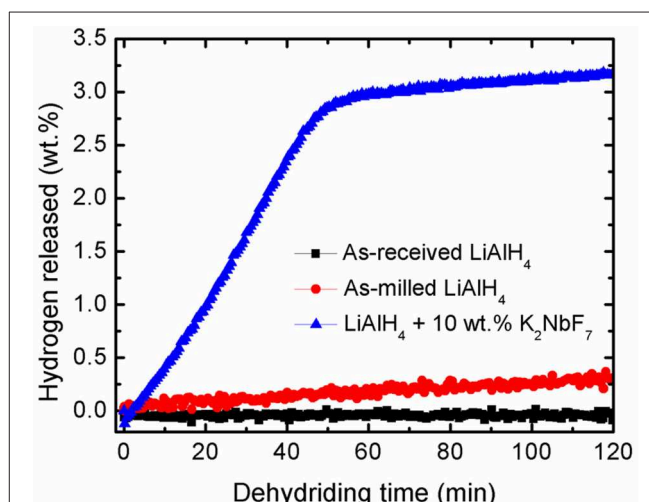


FIGURE 2 | Dehydrating kinetics curves of as-received LiAlH₄, as-milled LiAlH₄, and LiAlH₄ + 10 wt.% K₂NbF₇ at 90°C.

Further study on the catalytic activity of K₂NbF₇ was performed based on the desorption kinetics experiment. **Figure 2** depicts a comparison of the hydrogen desorption at 90°C for LiAlH₄ and LiAlH₄ modified by the addition of 10 wt.% K₂NbF₇. It is noticeable that within 120 min, the undoped LiAlH₄ was only able to desorb a small amount of hydrogen; 0.1 wt.% for the as-received LiAlH₄ and 0.4 wt.% for the as-milled LiAlH₄. Surprisingly, with the addition of 10 wt.% K₂NbF₇, the doped sample desorbed ~3.2 wt.% H₂ within the same duration. This desorption rate was 30 times faster than that of the as-received LiAlH₄. This enhancement may be correlated to the formation of surface defects and active materials through the reaction of the LiAlH₄ + 10 wt.% K₂NbF₇ composite (Cai et al., 2016).

In terms of thermal behavior, DSC experiments were conducted for the doped and un-doped LiAlH₄ samples. **Figure 3**

displays the DSC curves of the samples at a heating ramp of 15°C/min. Both the doped and un-doped LiAlH₄ have two endothermic and exothermic peaks. The first exothermic peak corresponds to the reaction of LiAlH₄ with surface hydroxyl groups, while the first endothermic peak is ascribed as its melting process. The second exothermic peak is attributed to the decomposition of LiAlH₄, as described in Equation (1), and the second endothermic peak correlates with the decomposition of Li₃AlH₆, as described by Equation (2). Both samples exhibit similar thermal behavior, but the peaks of the LiAlH₄ + 10 wt.% K₂NbF₇ sample occur at a lower temperature as compared to as-milled LiAlH₄.

Fundamentally, the enhancement of the initial temperature to release hydrogen and the faster desorption kinetics rates are correlated with the energy barrier of LiAlH₄. In this study, the decomposition activation energy (E_A) is the least possible amount of energy needed by LiAlH₄ to begin the hydrogen desorption

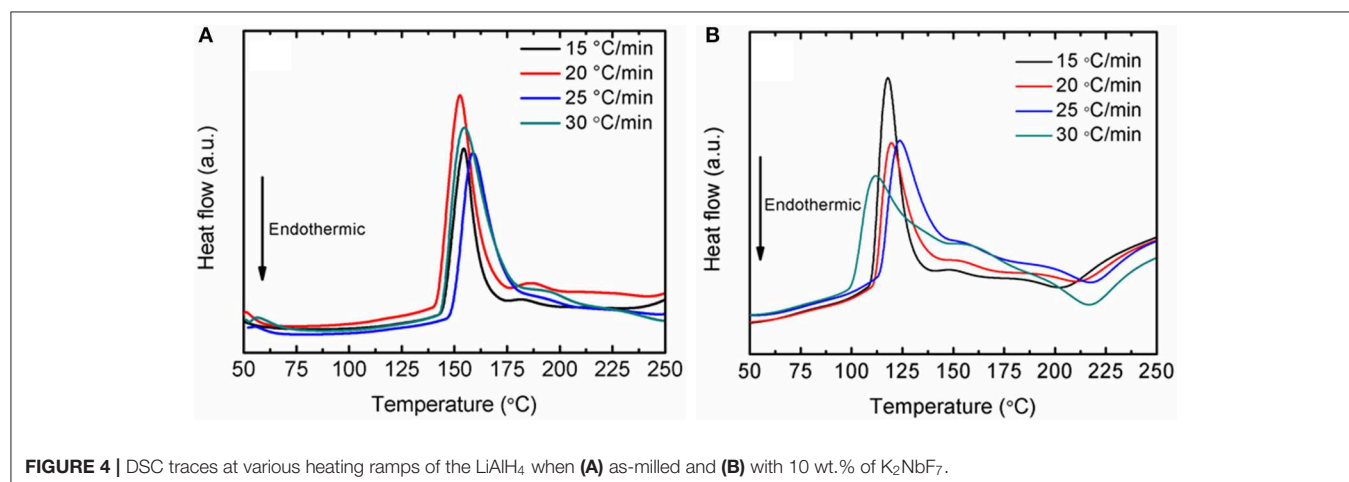
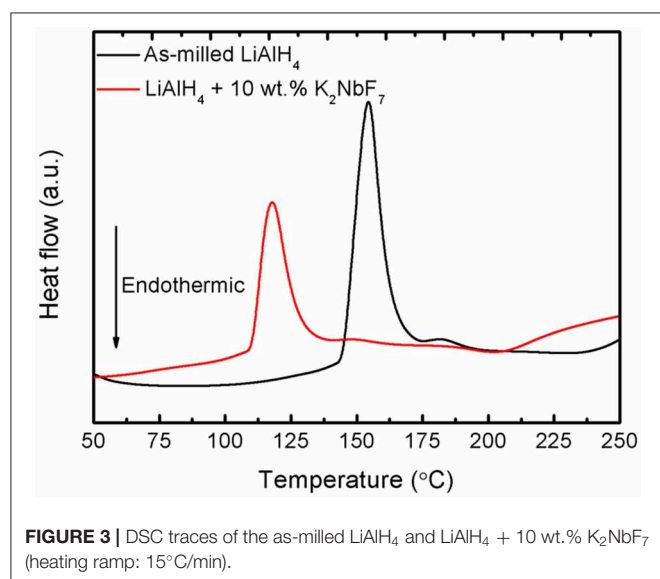
process. **Figure 4** shows DSC traces for several heating ramps (15, 20, 25, and 25°C/min). By referring to the plots, the activation energies for both decomposition stages of the as-milled LiAlH₄ and LiAlH₄ + 10 wt.% K₂NbF₇ samples were determined using the Kissinger analysis, as in equation (4):

$$\ln [\beta / T_p^2] = -E_A / RT_p + A \quad (4)$$

where β , T_p , R , and A are the heating rate, peak temperature in the DSC curve, gas constant, and linear constant, respectively. The apparent activation energy was determined from the slope of $\ln [\beta / T_p^2]$ versus $1000/T_p$, as shown in **Figure 5**.

The activation energy was calculated based on the second exothermic (decomposition of LiAlH₄) and second endothermic (decomposition of Li₃AlH₆) reactions. For the as-milled LiAlH₄, the activation energy values were 104 and 112 kJ/mol for the first two stages of reaction, respectively. After the addition of 10 wt.% K₂NbF₇, the activation energy values dropped to 80 kJ/mol (first stage) and 86 kJ/mol (second stage), 23% lower than those of the un-doped LiAlH₄. These results are in good agreement with other studies that prove the addition of a catalyst is able to reduce the activation energy of LiAlH₄. **Table 1** lists the activation energy from previous studies for comparison purposes. The reduction in these activation energies verifies that K₂NbF₇ plays a major role in enhancing the desorption kinetics performance of LiAlH₄.

The morphological structures of the doped and un-doped LiAlH₄ were examined using SEM equipment. **Figure 6** shows SEM images of the un-doped and doped-LiAlH₄ samples. As shown in **Figure 6**, the pure LiAlH₄ exhibits larger particle sizes than the milled sample. The as-received LiAlH₄ (**Figure 6A**) has larger (15–40 μm), non-uniform rod-shaped particles. Furthermore, the as-received LiAlH₄ shows a uniform size distribution and consists of “blocky” particles, consistent with the report by Varin and Zbroniec (2010). Meanwhile, after 1 hour of milling, the milled LiAlH₄ (**Figure 6B**) displays a reduction in particle sizes but with some agglomeration and inconsistency in particle size. Then, with the addition of 10 wt.% of K₂NbF₇ (**Figure 6C**), the morphological structure of the sample was notably enhanced. The doped sample has smaller



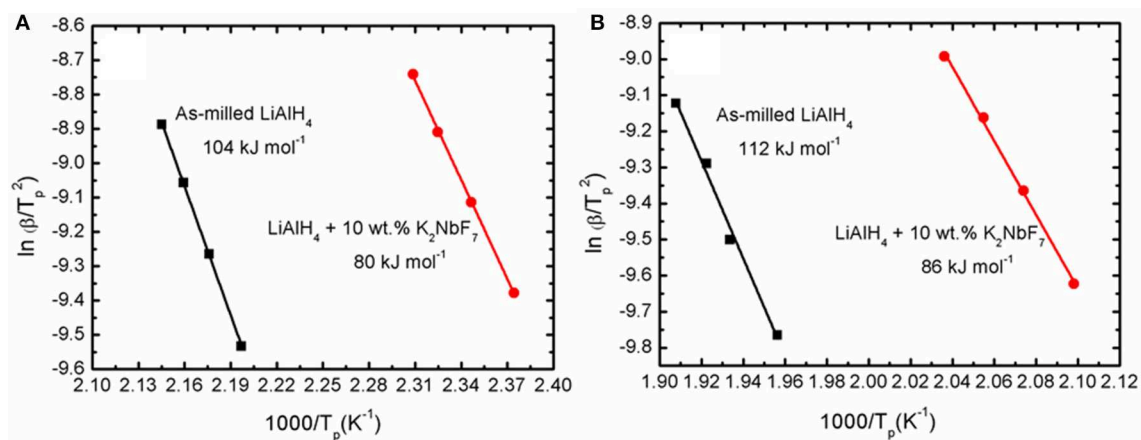


FIGURE 5 | Corresponding Kissinger plots of the as-milled LiAlH₄ and LiAlH₄ + 10 wt.% K₂NbF₇ for the (A) first stage and (B) second stage of reaction.

TABLE 1 | Activation energy of catalyst-doped LiAlH₄ from previous studies.

System	Activation energy (kJ/mol)		References
	First stage	Second stage	
LiAlH ₄ +K ₂ TiF ₆	78.20	90.80	Li et al., 2012
LiAlH ₄ +Ti ₃ C ₂	79.81	99.68	Xia et al., 2019
LiAlH ₄ +FeCl ₂	81.48	105.01	Cai et al., 2016
LiAlH ₄ +ScCl ₃	82.30	93.20	Cao et al., 2018
LiAlH ₄ +Co@C	95.36	115.60	Li et al., 2015

particle sizes and is less agglomerated. This observation is in line with numerous research results that have shown a reduction of particle sizes with the addition of a catalyst (Aguey-Zinsou et al., 2007; Ali et al., 2018; Yahya M. and and Ismail M., 2018). In this study, K₂NbF₇ functioned as a dispersing agent that impeded the sample from agglomerating. The particle size is important because smaller particles provide more area for surface defects and additional grain boundaries (Schulz et al., 1999; Sakintuna et al., 2007; Ranjbar et al., 2009). As a consequence, the desorption kinetics of LiAlH₄ will be improved.

Figure 7 presents the XRD profiles of the as-received LiAlH₄, as-milled LiAlH₄, and LiAlH₄-K₂NbF₇ sample. The XRD characterization was performed to explore the reaction process and the mechanism that operated during the milling process. **Figure 7A** displays the XRD pattern of the as-received LiAlH₄ and shows that only the LiAlH₄ phase was detected, which confirms the purity of the LiAlH₄. The XRD pattern of the milled LiAlH₄ **Figure 7B** shows similar peaks to the as-received LiAlH₄. This result shows that LiAlH₄ has high stability during the milling process and agrees well with a previous study (Ismail et al., 2010). Meanwhile, with the addition of 10 wt.% of K₂NbF₇ (**Figure 7C**), only LiAlH₄ and Al peaks are visible and no peak of K₂NbF₇ was detected, suggesting that the amount of catalyst was too small to be picked up by the XRD. The appearance of Al peaks indicates that a part of the LiAlH₄ had decomposed

to Li₃AlH₆ and Al (reaction 1) during the milling process in the presence of 10 wt.% K₂NbF₇. Surprisingly, the XRD result for the 10 wt.% K₂NbF₇-doped LiAlH₄ sample does not show any peaks of Li₃AlH₆. Additional characterization was carried out for a doped sample with 30 wt.% K₂NbF₇ (**Figure 7D**). A K₂NbF₇ peak was against not detected by the XRD for this sample. This may be because the K₂NbF₇ is in an amorphous state. Similar phenomena were reported by previous studies, where several catalysts like TiO₂ and TiF₃ were not detected by the XRD after the milling process (Ismail et al., 2011; Zang et al., 2015). However, for the LiAlH₄ + 30 wt.% K₂NbF₇ sample, diffraction peaks corresponding to the decomposition product, Al and Li₃AlH₆, were detected. Meanwhile, unlike for the LiAlH₄ + 10 wt.% K₂NbF₇ sample, for which only peaks of Al were detected while peaks of Li₃AlH₆ could not be discovered by XRD.

Figure 8 shows the IR spectra of the as-received LiAlH₄, as-milled LiAlH₄, and LiAlH₄ + 10 wt.% K₂NbF₇ in the range of 800 to 2,000 cm⁻¹. The FTIR characterizations were conducted to identify the presence of Li₃AlH₆ in the 10 wt.% K₂NbF₇-doped LiAlH₄ sample. For all samples, two distinct regions of Al-H modes were detected at around 800–900 cm⁻¹ ([AlH₄]⁻ stretching modes) and 1,600–1,800 cm⁻¹ ([AlH₄]⁻ bending modes), respectively. Furthermore, with the addition of 10 wt.% K₂NbF₇, a weak IR absorption peak at 1,398 cm⁻¹ was detected, which indicates the presence of Li₃AlH₆. This result suggests that with the addition of 10 wt.% K₂NbF₇, LiAlH₄ was partially decomposed to Li₃AlH₆ and Al (reaction 1) during the milling process, consistent with the XRD results (**Figure 7C**).

To investigate the specific mechanism that is related to the enhanced desorption performance of LiAlH₄, the dehydrogenated sample was examined using XRD. The XRD pattern for the dehydrogenated sample is depicted in **Figure 9**. After the dehydrogenation process at 250°C, the main peaks observed are the LiAlH₄ dehydrogenation products, LiH and Al, which indicates complete dehydrogenation of LiAlH₄. In addition, peaks for LiF and NbF₄ were detected after the dehydrogenation process. However, the peak of the K-containing

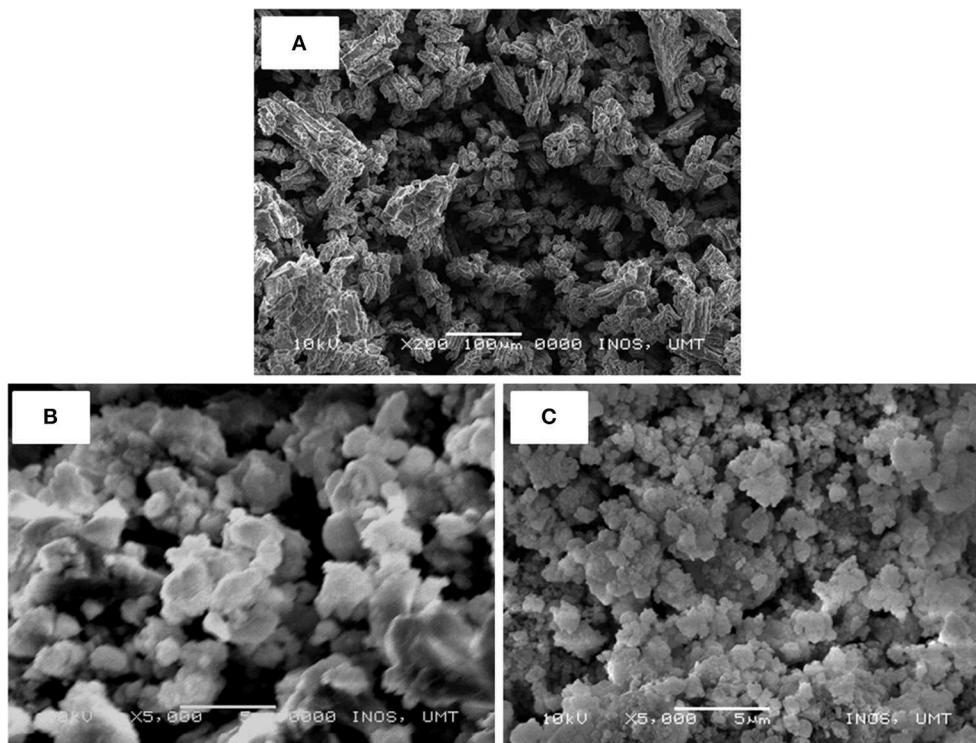


FIGURE 6 | SEM images of LiAlH₄ when (A) as-received, (B) as-milled, and (C) with 10 wt.% of K₂NbF₇.

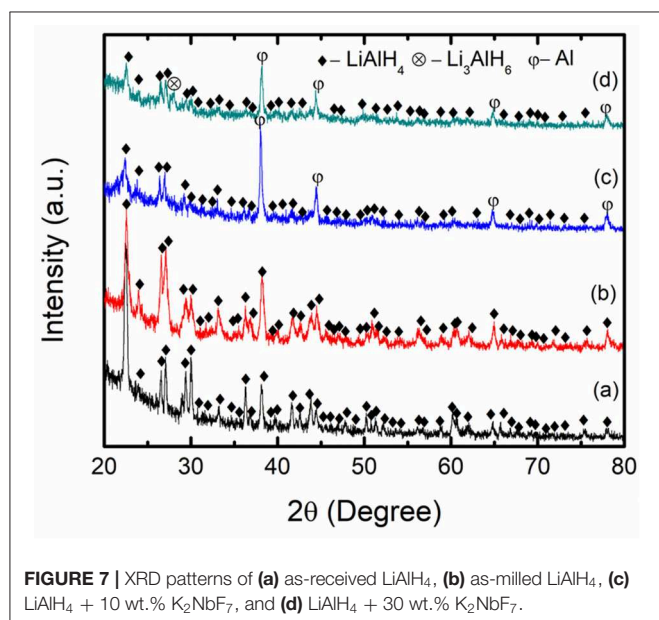


FIGURE 7 | XRD patterns of (a) as-received LiAlH₄, (b) as-milled LiAlH₄, (c) LiAlH₄ + 10 wt.% K₂NbF₇, and (d) LiAlH₄ + 30 wt.% K₂NbF₇.

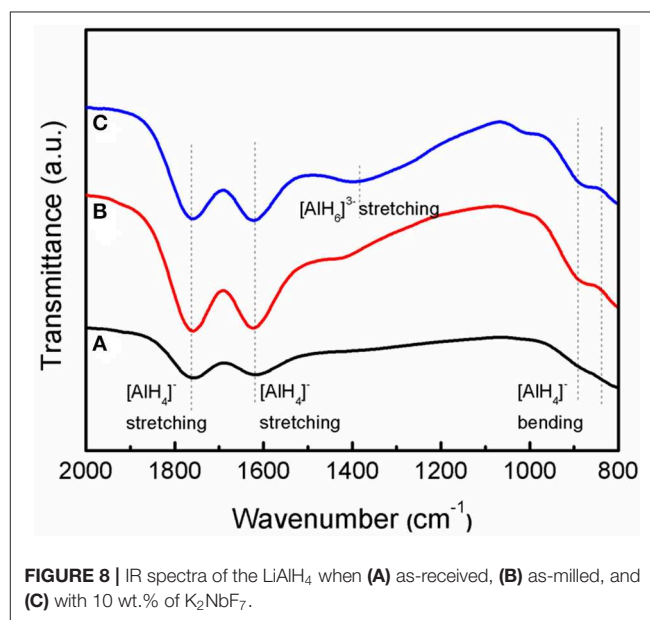
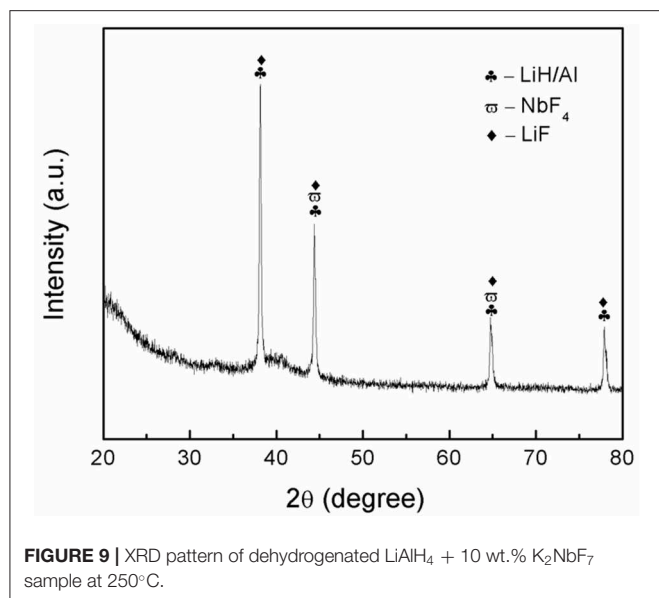


FIGURE 8 | IR spectra of the LiAlH₄ when (A) as-received, (B) as-milled, and (C) with 10 wt.% of K₂NbF₇.

phase was not detected after the dehydrogenation process, potentially due to the low amount of catalyst.

Niobium fluoride is well established as a promising catalyst that plays a vital role in enhancing the hydrogenation performance of solid-state material (Luo et al., 2007; Malka et al.,

2011; Mao et al., 2013). It is reasonable to state that the NbF₄ that formed *in situ* after the desorption process contributes to a remarkable amelioration of the desorption behavior of LiAlH₄. This result well-agreed with previous research that demonstrates the outstanding dehydrogenation performance of LiAlH₄-NbF₅



(Ismail et al., 2010). On the other hand, the LiF formed was believed to significantly affect the hydrogenation behavior of the doped sample based on work carried out as by Gosalawit-Utke et al. (2010). Additionally, it is believed that the formation of LiF plays a similar role in the growth of LiH and Al, since LiF has a similar cubic structure (space group: Fm-3m; Y. Liu et al., 2010). Also, LiF crystallites act as nucleation sites and facilitate the growth of LiH and Al crystallites, which promotes to the change of the nucleation morphology. These two factors significantly contribute to the kinetics enhancement achieved in the doped sample. Additionally, it is believed that K or K-containing phases also play a vital role in enhancing the desorption behavior of LiAlH₄. This was deduced based on successful previous work on the application of K as a catalyst for solid-state materials (Wang et al., 2009; Dong et al., 2014). Therefore, it can be concluded that the *in situ* formation of LiF, NbF₄, and K or K-containing phases synergistically contributed to the amelioration of the dehydrogenation kinetics of LiAlH₄.

REFERENCES

- Aguey-Zinsou, K. F., Fernandez, J. A., Klassen, T., and Bormann, R. (2007). Effect of Nb₂O₅ on MgH₂ properties during mechanical milling. *Int. J. Hydrogen Energy* 32, 2400–2407. doi: 10.1016/j.ijhydene.2006.10.068
- Ali, N. A., Idris, N. H., Din, M. F. M., Mustafa, N. S., Sazelee, N. A., Halim Yap, F. A., et al. (2018). Nanolayer-like-shaped MgFe₂O₄ synthesized via a simple hydrothermal method and its catalytic effect on the hydrogen storage properties of MgH₂. *RSC Adv.* 8, 15667–15674. doi: 10.1039/C8RA02168F
- Ali, N. A., Idris, N. H., Sazelee, N. A., Yahya, M. S., Yap, F. A. H., and Ismail, M. (2019). Catalytic effects of MgFe₂O₄ addition on the dehydrogenation properties of LiAlH₄. *Int. J. Hydrogen Energy* 44, 28227–28234. doi: 10.1016/j.ijhydene.2019.09.083
- Amama, P. B., Grant, J. T., Shamberger, P. J., Voevodin, A. A., and Fisher, T. S. (2012). Improved dehydrogenation properties of Ti-doped LiAlH₄: role of Ti precursors. *J. Phys. Chem. C* 116, 21886–21894. doi: 10.1021/jp307225w

CONCLUSION

K₂NbF₇ demonstrated an excellent catalytic effect on the desorption behavior of LiAlH₄. The initial temperatures at which LiAlH₄ + 10 wt.% K₂NbF₇ released hydrogen, 90 and 149°C for the first two stages, were lower than those of the as-milled LiAlH₄ (147 and 175°C). In terms of desorption kinetics behavior, the LiAlH₄ + 10 wt.% K₂NbF₇ released 3.2 wt.% of hydrogen within 120 min, which is 30 faster than the pure LiAlH₄. The addition of K₂NbF₇ significantly reduced the decomposition activation energy from 104 to 80 kJ/mol for the first stage and 112 to 86 kJ/mol for the second stage. The XRD spectra suggested that the *in situ* formation of LiF, NbF₄, and K or K-containing phases acted as boosters and ameliorated the dehydrogenation behavior of LiAlH₄. This work demonstrates that K₂NbF₇ has a superior catalytic effect and confers better desorption behavior to LiAlH₄.

DATA AVAILABILITY STATEMENT

The datasets generated for this study are available on request to the corresponding author.

AUTHOR CONTRIBUTIONS

All authors listed have made a substantial, direct and intellectual contribution to the work, and approved it for publication.

FUNDING

This work was financially supported by Golden Goose Research Grant (GGRG) VOT 55190, Universiti Malaysia Terengganu.

ACKNOWLEDGMENTS

The authors would like to acknowledge Universiti Malaysia Terengganu for providing complete facilities at which to perform this research.

- Andrei, C., Walmsley, J., Blanchard, D., Brinks, H., Holmestad, R., and Hauback, B. (2005). Electron microscopy studies of lithium aluminum hydrides. *J. Alloy. Compd.* 395, 307–312. doi: 10.1016/j.jallcom.2004.11.058
- Ares, J., Aguey-Zinsou, K. F., Porcu, M., Sykes, J., Dornheim, M., Klassen, T., et al. (2008). Thermal and mechanically activated decomposition of LiAlH₄. *Mater. Res. Bull.* 43, 1263–1275. doi: 10.1016/j.materresbull.2007.05.018
- Balema, V., Pecharsky, V., and Dennis, K. (2000). Solid state phase transformations in LiAlH₄ during high-energy ball-milling. *J. Alloy. Compd.* 313, 69–74. doi: 10.1016/S0925-8388(00)01201-9
- Balema, V., Wiench, J., Dennis, K., Pruski, M., and Pecharsky, V. (2001). Titanium catalyzed solid-state transformations in LiAlH₄ during high-energy ball-milling. *J. Alloy. Compd.* 329, 108–114. doi: 10.1016/S0925-8388(01)01570-5
- Barthelemy, H., Weber, M., and Barbier, F. (2017). Hydrogen storage: recent improvements and industrial perspectives. *Int. J. Hydrogen Energy* 42, 7254–7262. doi: 10.1016/j.ijhydene.2016.03.178

- Cai, J., Zang, L., Zhao, L., Liu, J., and Wang, Y. (2016). Dehydrogenation characteristics of LiAlH₄ improved by *in-situ* formed catalysts. *J. Energy Chem.* 25, 868–873. doi: 10.1016/j.jchem.2016.06.004
- Cao, Z., Ma, X., Wang, H., and Ouyang, L. (2018). Catalytic effect of ScCl₃ on the dehydrogenation properties of LiAlH₄. *J. Alloys Compd.* 762, 73–79. doi: 10.1016/j.jallcom.2018.05.213
- Cheng, C., Chen, M., Xiao, X., Huang, X., Zheng, J., and Chen, L. (2018). Superior reversible hydrogen storage properties and mechanism of LiBH₄-MgH₂-Al doped with NbF₅ additive. *J. Phys. Chem. C* 122, 7613–7620. doi: 10.1021/acs.jpcc.8b00959
- Crabtree, G. W., Dresselhaus, M. S., and Buchanan, M. V. (2004). The hydrogen economy. *Phys. Today* 57, 39–44. doi: 10.1063/1.1878333
- Dalebrook, A. F., Gan, W., Grasemann, M., Moret, S., and Laurency, G. (2013). Hydrogen storage: beyond conventional methods. *Chem. Commun.* 49, 8735–8751. doi: 10.1039/c3cc43836h
- Dong, B. X., Song, L., Teng, Y. L., Ge, J., and Zhang, S. Y. (2014). Enhanced hydrogen desorption reaction kinetics by optimizing the reaction conditions and doping potassium compounds in the LiH–NH₃ system. *Int. J. Hydrogen Energy* 39, 13838–13843. doi: 10.1016/j.ijhydene.2014.03.005
- Fernandez, J. A., Aguey-Zinsou, F., Elsaesser, M., Ma, X., Dornheim, M., Klassen, T., et al. (2007). Mechanical and thermal decomposition of LiAlH₄ with metal halides. *Int. J. Hydrogen Energy* 32, 1033–1040. doi: 10.1016/j.ijhydene.2006.07.011
- Gosalawit-Utke, R., Bellosta von Colbe, J. M., Dornheim, M., Jensen, T. R., Cerenius, Y., Bonatto Minella, C., et al. (2010). LiF–MgB₂ system for reversible hydrogen storage. *J. Phys. Chem. C* 114, 10291–10296. doi: 10.1021/jp910266m
- Ismail, M., Zhao, Y., Yu, X. B., and Dou, S. X. (2010). Effects of NbF₅ addition on the hydrogen storage properties of LiAlH₄. *Int. J. Hydrogen Energy* 35, 2361–2367. doi: 10.1016/j.ijhydene.2009.12.178
- Ismail, M., Zhao, Y., Yu, X. B., Nevirkovets, I. P., and Dou, S. X. (2011). Significantly improved dehydrogenation of LiAlH₄ catalysed with TiO₂ nanopowder. *Int. J. Hydrogen Energy* 36, 8327–8334. doi: 10.1016/j.ijhydene.2011.04.074
- Kou, H., Sang, G., Zhou, Y., Wang, X., Huang, Z., Luo, W., et al. (2014). Enhanced hydrogen storage properties of LiBH₄ modified by NbF₅. *Int. J. Hydrogen Energy* 39, 11675–11682. doi: 10.1016/j.ijhydene.2014.05.179
- Langmi, H. W., McGrady, G. S., Liu, X., and Jensen, C. M. (2010). Modification of the H₂ desorption properties of LiAlH₄ through doping with Ti. *J. Phys. Chem. C* 114, 10666–10669. doi: 10.1021/jp102641p
- Li, L., An, C., Wang, Y., Xu, Y., Qiu, F., Wang, Y., et al. (2014). Enhancement of the H₂ desorption properties of LiAlH₄ doping with NiCo₂O₄ nanorods. *Int. J. Hydrogen Energy* 39, 4414–4420. doi: 10.1016/j.ijhydene.2013.12.210
- Li, L., Qiu, F., Wang, Y., Xu, Y., An, C., Liu, G., et al. (2013). Enhanced hydrogen storage properties of TiN–LiAlH₄ composite. *Int. J. Hydrogen Energy* 38, 3695–3701. doi: 10.1016/j.ijhydene.2013.01.088
- Li, L., Wang, Y., Jiao, L., and Yuan, H. (2015). Enhanced catalytic effects of Co@C additive on dehydrogenation properties of LiAlH₄. *J. Alloys Compd.* 645(Suppl.1), S468–S471. doi: 10.1016/j.jallcom.2014.12.080
- Li, Z., Li, P., Wan, Q., Zhai, F., Liu, Z., Zhao, K., et al. (2013). Dehydrogenation improvement of LiAlH₄ catalyzed by Fe₂O₃ and Co₂O₃ nanoparticles. *J. Phys. Chem. C* 117, 18343–18352. doi: 10.1021/jp405844z
- Li, Z., Liu, S., Si, X., Zhang, J., Jiao, C., Wang, S., et al. (2012). Significantly improved dehydrogenation of LiAlH₄ destabilized by K₂TiF₆. *Int. J. Hydrogen Energy* 37, 3261–3267. doi: 10.1016/j.ijhydene.2011.10.038
- Liu, S., Ma, Q., Lü, H., Zheng, X., Feng, X., Xiao, G., et al. (2014). Study on hydrogen release capacity of LiAlH₄ doped with CeO₂. *Rare Metal. Mat. Eng.* 43, 544–547. doi: 10.1016/S1875-5372(14)60073-4
- Liu, S. S., Sun, L. X., Zhang, Y., Xu, F., Zhang, J., Chu, H. L., et al. (2009). Effect of ball milling time on the hydrogen storage properties of TiF₃-doped LiAlH₄. *Int. J. Hydrogen Energy* 34, 8079–8085. doi: 10.1016/j.ijhydene.2009.07.090
- Liu, X., Beattie, S. D., Langmi, H. W., McGrady, G. S., and Jensen, C. M. (2012). Ti-doped LiAlH₄ for hydrogen storage: rehydrogenation process, reaction conditions and microstructure evolution during cycling. *Int. J. Hydrogen Energy* 37, 10215–10221. doi: 10.1016/j.ijhydene.2012.04.018
- Liu, Y., Wang, F., Cao, Y., Gao, M., Pan, H., and Wang, Q. (2010). Mechanisms for the enhanced hydrogen desorption performance of the TiF₄-catalyzed Na₂LiAlH₆ used for hydrogen storage. *Energy Environ. Sci.* 3, 645–653. doi: 10.1039/b920270f
- Luo, Y., Wang, P., Ma, L. P., and Cheng, H. M. (2007). Enhanced hydrogen storage properties of MgH₂ co-catalyzed with NbF₅ and single-walled carbon nanotubes. *Scripta Mater.* 56, 765–768. doi: 10.1016/j.scriptamat.2007.01.016
- Luo, Y., Wang, P., Ma, L. P., and Cheng, H. M. (2008). Hydrogen sorption kinetics of MgH₂ catalyzed with NbF₅. *J. Alloys Compd.* 453, 138–142. doi: 10.1016/j.jallcom.2006.11.113
- Malka, I., Pisarek, M., Czujko, T., and Bystrzycki, J. (2011). A study of the ZrF₄, NbF₅, TaF₅, and TiCl₃ influences on the MgH₂ sorption properties. *Int. J. Hydrogen Energy* 36, 12909–12917. doi: 10.1016/j.ijhydene.2011.07.020
- Mao, J., Guo, Z., Yu, X., and Liu, H. (2013). Combined effects of hydrogen back-pressure and NbF₅ addition on the dehydrogenation and rehydrogenation kinetics of the LiBH₄-MgH₂ composite system. *Int. J. Hydrogen Energy* 38, 3650–3660. doi: 10.1016/j.ijhydene.2012.12.106
- Parra, D., Valverde, L., Pino, F. J., and Patel, M. K. (2019). A review on the role, cost and value of hydrogen energy systems for deep decarbonisation. *Renew. Sust. Energy Rev.* 101, 279–294. doi: 10.1016/j.rser.2018.11.010
- Pukazhvelan, D., Kumar, V., and Singh, S. (2012). High capacity hydrogen storage: basic aspects, new developments and milestones. *Nano Energy* 1, 566–589. doi: 10.1016/j.nanoen.2012.05.004
- Ranjbar, A., Guo, Z., Yu, X., Wexler, D., Calka, A., Kim, C., et al. (2009). Hydrogen storage properties of MgH₂-SiC composites. *Mater. Chem. Phys.* 114, 168–172. doi: 10.1016/j.matchemphys.2008.09.001
- Resan, M., Hampton, M. D., Lomness, J. K., and Slattery, D. K. (2005). Effects of various catalysts on hydrogen release and uptake characteristics of LiAlH₄. *Int. J. Hydrogen Energy* 30, 1413–1416. doi: 10.1016/j.ijhydene.2004.12.009
- Sakintuna, B., Lamari-Darkrim, F., and Hirscher, M. (2007). Metal hydride materials for solid hydrogen storage: a review. *Int. J. Hydrogen Energy* 32, 1121–1140. doi: 10.1016/j.ijhydene.2006.11.022
- Sazelee, N., Yahya, M., Idris, N., Din, M. M., and Ismail, M. (2019). Desorption properties of LiAlH₄ doped with LaFeO₃ catalyst. *Int. J. Hydrogen Energy* 44, 11953–11960. doi: 10.1016/j.ijhydene.2019.03.102
- Schulz, R., Huot, J., Liang, G., Boily, S., Lalande, G., Denis, M., et al. (1999). Recent developments in the applications of nanocrystalline materials to hydrogen technologies. *Mater. Sci. Eng. A* 267, 240–245. doi: 10.1016/S0921-5093(99)00098-2
- Sulaiman, N., and Ismail, M. (2017). Catalytic effect of SrFe₁₂O₁₉ on the hydrogen storage properties of LiAlH₄. *Int. J. Hydrogen Energy* 42, 19126–19134. doi: 10.1016/j.ijhydene.2017.06.005
- Sulaiman, N., Mustafa, N., and Ismail, M. (2016). Effect of Na₃FeF₆ catalyst on the hydrogen storage properties of MgH₂. *Dalton Trans.* 45, 7085–7093. doi: 10.1039/C6DT00068A
- Sun, T., Huang, C., Wang, H., Sun, L., and Zhu, M. (2008). The effect of doping NiCl₂ on the dehydrogenation properties of LiAlH₄. *Int. J. Hydrogen Energy* 33, 6216–6221. doi: 10.1016/j.ijhydene.2008.08.027
- Suttisawat, Y., Rangsunvigit, P., Kitiyanan, B., Muangsin, N., and Kulprathipanja, S. (2007). Catalytic effect of Zr and Hf on hydrogen desorption/absorption of NaAlH₄ and LiAlH₄. *Int. J. Hydrogen Energy* 32, 1277–1285. doi: 10.1016/j.ijhydene.2006.07.020
- Varin, R., and Zbroniec, L. (2010). Decomposition behavior of unmilled and ball milled lithium alanate (LiAlH₄) including long-term storage and moisture effects. *J. Alloy. Compd.* 504, 89–101. doi: 10.1016/j.jallcom.2010.05.059
- Varin, R. A., and Parviz, R. (2012). The effects of the micrometric and nanometric iron (Fe) additives on the mechanical and thermal dehydrogenation of lithium alanate (LiAlH₄), its self-discharge at low temperatures and rehydrogenation. *Int. J. Hydrogen Energy* 37, 9088–9102. doi: 10.1016/j.ijhydene.2012.02.182
- Wang, J., Liu, T., Wu, G., Li, W., Liu, Y., Araújo, C. M., et al. (2009). Potassium-modified Mg(NH₂)₂/LiH system for hydrogen storage. *Angew. Chem. Int. Ed.* 48, 5828–5832. doi: 10.1002/anie.200805264
- Wang, X., Xiao, X., Zheng, J., Huang, X., Chen, M., and Chen, L. (2020). *In-situ* synthesis of amorphous Mg(BH₄)₂ and chloride composite modified by NbF₅ for superior reversible hydrogen storage properties. *Int. J. Hydrogen Energy* 45, 2044–2053. doi: 10.1016/j.ijhydene.2019.11.023
- Winter, C. J. (2009). Hydrogen energy—abundant, efficient, clean: a debate over the energy-system-of-change. *Int. J. Hydrogen Energy* 34, S1–S2. doi: 10.1016/j.ijhydene.2009.05.063
- Wohlwend, J. L., Amama, P. B., Shamberger, P. J., Varshney, V., Roy, A. K., and Fisher, T. S. (2012). Effects of Titanium-containing additives on the

- dehydrogenation properties of LiAlH₄: a computational and experimental study. *J. Phys. Chem. C* 116, 22327–22335. doi: 10.1021/jp3050109
- Xia, Y., Zhang, H., Sun, Y., Sun, L., Xu, F., Sun, S., et al. (2019). Dehybridization effect in improved dehydrogenation of LiAlH₄ by doping with two-dimensional Ti₃C₂. *Mater. Today Nano.* 8:100054. doi: 10.1016/j.mtnano.2019.100054
- Xiao, X., Shao, J., Chen, L., Kou, H., Fan, X., Deng, S., et al. (2012). Effects of NbF₅ addition on the de/rehydrogenation properties of 2LiBH₄/MgH₂ hydrogen storage system. *Int. J. Hydrogen Energy* 37, 13147–13154. doi: 10.1016/j.ijhydene.2012.03.140
- Xueping, Z., Ping, L., Humail, I., Fuqiang, A., Guoqing, W., and Xuanhui, Q. (2007). Effect of catalyst LaCl₃ on hydrogen storage properties of lithium alanate (LiAlH₄). *Int. J. Hydrogen Energy* 32, 4957–4960. doi: 10.1016/j.ijhydene.2007.06.031
- Xueping, Z., Ping, L., and Xuanhui, Q. (2009). Effect of additives on the reversibility of lithium alanate (LiAlH₄). *Rare. Metal Mat. Eng.* 38, 766–769. doi: 10.1016/S1875-5372(10)60034-3
- Yahya, M., and Ismail, M. (2018). Synergistic catalytic effect of SrTiO₃ and Ni on the hydrogen storage properties of MgH₂. *Int. J. Hydrogen Energy* 43, 6244–6255. doi: 10.1016/j.ijhydene.2018.02.028
- Yahya, M. S., and Ismail, M. (2018). Improvement of hydrogen storage properties of MgH₂ catalyzed by K₂NbF₇ and multiwall carbon nanotube. *J. Phys. Chem. C* 122, 11222–11233. doi: 10.1021/acs.jpcc.8b02162
- Yahya, M. S., Sulaiman, N. N., Mustafa, N. S., Halim Yap, F. A., and Ismail, M. (2018). Improvement of hydrogen storage properties in MgH₂ catalysed by K₂NbF₇. *Int. J. Hydrogen Energy* 43, 14532–14540. doi: 10.1016/j.ijhydene.2018.05.157
- Yap, F. H., Yahya, M., and Ismail, M. (2017). Enhancement of hydrogen storage properties in 4MgH₂-Na₃AlH₆ composite catalyzed by TiF₃. *Int. J. Hydrogen Energy* 42, 21096–21104. doi: 10.1016/j.ijhydene.2017.07.012
- Youn, J. S., Phan, D. T., Park, C. M., and Jeon, K. J. (2017). Enhancement of hydrogen sorption properties of MgH₂ with a MgF₂ catalyst. *Int. J. Hydrogen Energy* 42, 20120–20124. doi: 10.1016/j.ijhydene.2017.06.130
- Zang, L., Cai, J., Zhao, L., Gao, W., Liu, J., and Wang, Y. (2015). Improved hydrogen storage properties of LiAlH₄ by mechanical milling with TiF₃. *J. Alloys Compd.* 647, 756–762. doi: 10.1016/j.jallcom.2015.06.036
- Zhai, F., Li, P., Sun, A., Wu, S., Wan, Q., Zhang, W., et al. (2012). Significantly improved dehydrogenation of LiAlH₄ destabilized by MnFe₂O₄ nanoparticles. *J. Phys. Chem. C* 116, 11939–11945. doi: 10.1021/jp302721w
- Zhang, F., Zhao, P., Niu, M., and Maddy, J. (2016). The survey of key technologies in hydrogen energy storage. *Int. J. Hydrogen Energy* 41, 14535–14552. doi: 10.1016/j.ijhydene.2016.05.293

Conflict of Interest: The authors declare that the research was conducted in the absence of any commercial or financial relationships that could be construed as a potential conflict of interest.

Copyright © 2020 Ali, Sazelee, Yahya and Ismail. This is an open-access article distributed under the terms of the Creative Commons Attribution License (CC BY). The use, distribution or reproduction in other forums is permitted, provided the original author(s) and the copyright owner(s) are credited and that the original publication in this journal is cited, in accordance with accepted academic practice. No use, distribution or reproduction is permitted which does not comply with these terms.